Journal of Structural Geology, Vol. 14, No. 4, pp. 461 to 474, 1992
Printed in Great Britain

0191-8141/92 $05.00+0.00

Magnetic fabric as a structural indicator of the deformation path within a fold–thrust structure: a test case from the Corbières (NE Pyrenees, France)

OLIVIER AVERBUCH

Centre des Faibles Radioactivités, Laboratoire Mixte C.N.R.S.–C.E.A., Avenue de la Terrasse, 91198 Gif-sur-Yvette Cédex, France

DOMINIQUE FRIZON DE LAMOTTE

Laboratoire de Géologie Structurale, C.N.R.S. URA 1369, Université Paris-Sud, Bat. 504, 91405 Orsay Cédex, France

and

CATHERINE KISSEL

Centre des Faibles Radioactivités, Laboratoire Mixte C.N.R.S.–C.E.A., Avenue de la Terrasse, 91198 Gif-sur-Yvette Cédex, France

(*Received* 26 *June* 1991; *accepted in revised form* 30 *September* 1991)

Abstract—In order to define the deformation path and the distribution of internal deformation in a foreland fold–thrust structure, the anisotropy of magnetic susceptibility was measured in 150 samples taken from 11 sites throughout the Vitrollian sequence of the Lagrasse structure (most external Pyrenean Zone). Whereas surrounding rocks seem completely undeformed, the Vitrollian Formation exhibits a complete set of microstructural markers thereby allowing fault striation measurements at sites also sampled for magnetic fabric analysis. Structural analysis shows that two mechanisms acted successively during thrust motion. The first one resulted from a NW–SE layer parallel shortening (LPS). It was responsible for a well defined vertical magnetic foliation parallel to the regional cleavage, in which a vertical magnetic lineation developed in conjunction with an increase in the shortening intensity towards the zone which would subsequently fail, leading to the development of an imbricate thrust system. During this second event, internal deformation was concentrated around the hinge and in the forelimb of the frontal fold. Around the hinge, the magnetic lineation rotated to an horizontal NE–SW trend parallel to the fold axis, indicating a significant component of longitudinal stretching during the development of the frontal ramp-anticline. Subsequently, the magnetic lineation swung again and became parallel to the NW–SE tectonic transport direction beneath out-of-sequence forelimb thrusts. This complex deformation history is not accompanied by a linear increase in the degree of anisotropy. On the contrary, we observe a cycle of construction and destruction of the magnetic fabric during LPS and imbricate thrusting.

INTRODUCTION

THE last 20 years have seen an increase in the development of work focusing on the structure and the evolution of fold-and-thrust belts. This work has led to a better understanding of the geometry of fold–thrust structures (Dahlstrom 1969, Boyer & Elliot 1982 and to the generalization of analytic methods among which the balanced cross-section procedure is now commonly used both in academic and industrial work. Reliable use of such methods requires information about deformation mechanisms and particularly about the rate of internal distortion with respect to rigid-body translation and rotation (folding) (Hossack 1979). Geometric models of thrust sheet emplacement and strain distribution in thrust sheet have been proposed (Sanderson 1982, Suppe 1983). Testing of these models in the field requires the use of convenient strain markers. When they exist, as in the Scottish Caledonides (Coward & Kim 1981, Fischer & Coward 1982) or in the Appalachians (Wiltschko *et al.* 1985, Geiser 1988, Evans & Dunne 1991), a significant component of internal deformation is demonstrated.

However, these studies are not necessarily representative for the most external parts of the orogen, where strain markers are generally scarce, and rarely take into account deformation sequences. In order to discuss these crucial points, this paper aims to characterize the deformation path within a kilometric scale fold–thrust structure (the Lagrasse fold) from the most external part of the Pyrenean belt (SW France). We use a combination of structural and anisotropy of magnetic susceptibility (AMS) measurements. The latter method has proved to be a powerful way of detecting bulk preferred orientation of minerals and/or crystal lattices (Borradaile 1988). Thus it can provide useful information on strain state even in weakly deformed material (Kissel *et al.* 1986, Lowrie & Hirt 1987, Lee *et al.* 1990, Aubourg *et al.* 1991).

The Lagrasse structure provides, by the quality of the outcrops as well as by their distribution within the structure, a good opportunity for such work. An addi-

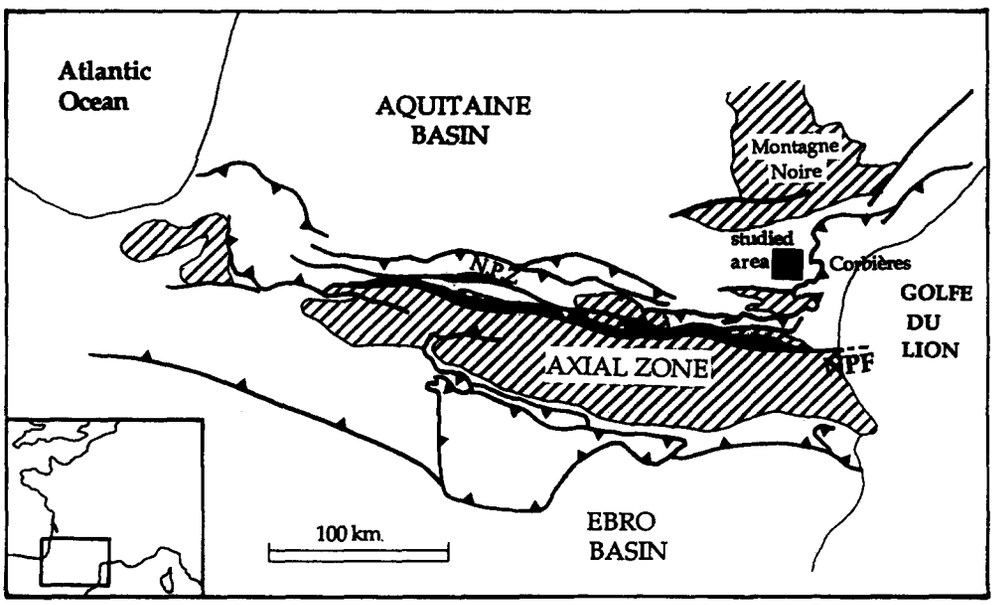

Fig. 1. Structural sketch map of the Pyrenees (after Roure *et al.* 1989). The black square indicates the studied area; dotted areas represent the Paleozoic basement; solid areas refer to high temperature–low pressure metamorphic zones; N.P.F.: North Pyrenean fault; N.P.Z.: North Pyrenean zone.

tional interest is the presence of a very peculiar formation, the Vitrollian fluviatile silts, in which both AMS measurements and structural analysis may be performed.

Before we present and discuss our results, we firstly propose a new structural interpretation of the Lagrasse fold.

THE LAGRASSE FOLD: GEOLOGICAL SETTING AND NEW STRUCTURAL INTERPRETATION

The Lagrasse fold lies in the foreland of the 'nappe des Corbières orientales' (Barrabé 1922), which joins the Languedoc fold–thrust belt and the North Pyrenean zone, forming an important orocline (Fig. 1). It involves a mostly Cenozoic sedimentary cover affected by numerous faults and hectometric to kilometric NE–SW-trending folds (Fig. 2).

The sedimentology and stratigraphy have been studied in detail within the region by Freytet (1970) and Plaziat (1984). The sedimentary succession consists of about 1000 m of essentially continental deposits of late Cretaceous to late Eocene age, comprising fluviatile silts and lacustrine limestones.

Palaeogeographically, the Lagrasse area corresponds to a transition zone between the Alaric Mountain to the north, in which the late Cretaceous formations (Maas-

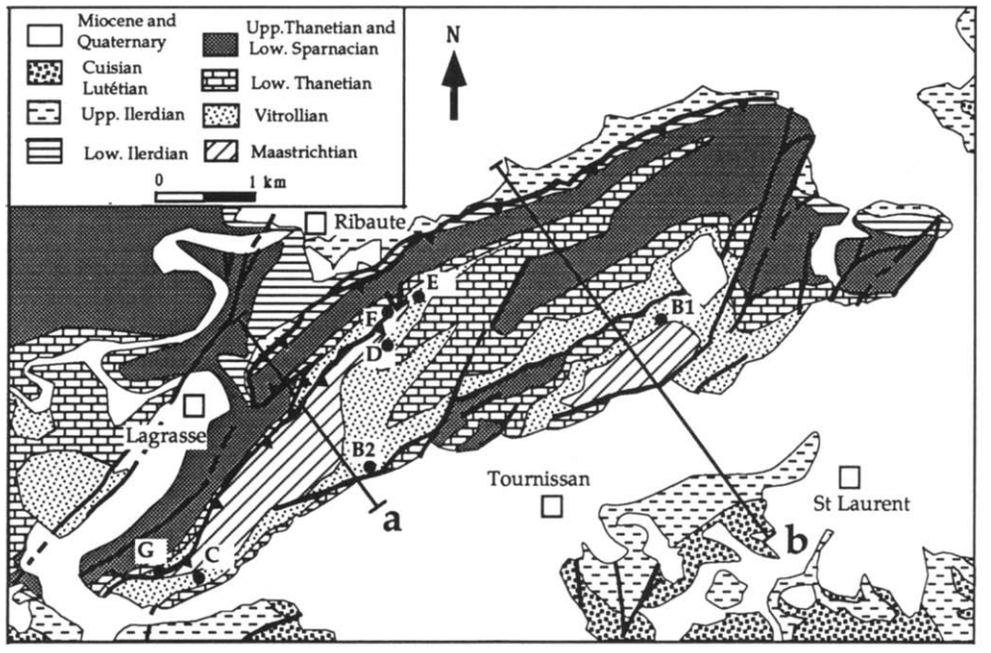

Fig. 2. Geological map of the Lagrasse fold (after Cluzel 1977, and Ellenberger *et al.* 1985). B1, B2, C, D, E, F and G refer to the sampled sites. The sites A1 and A2 are situated outside of the map, about 5 km west of Lagrasse. Section lines **a** and **b** refer to Fig. 4.

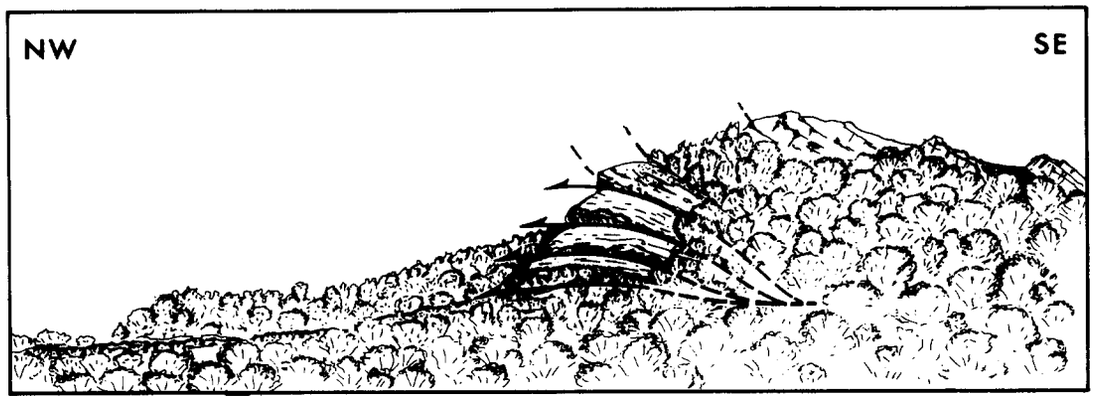

Fig. 3. The 'La Cagalière' duplex (drawing from a photograph).

trichtian lacustrine limestones and fluviatile deposits) lie directly on the deformed Palaeozoic basement, and the Boutenac Hills to the east where a consensed Mesozoic lithostratigraphic succession from Middle Trias to Upper Cretaceous is known. These rapid lateral variations prevent any precise extrapolation of the substratum composition under the outcropping part of the Lagrasse fold.

Ellenberger (1967) was the first to make a precise cartography and description of this structure (Fig. 2). He interpreted it as an asymmetric NW-verging kink flexure with an hectometric vertical (and sometimes reversed) short limb, and a kilometric horizontal roof limb. The short limb is cross-cut by several thrust faults, well developed in the southwestern part of the structure.

Concerning the microstructural imprints, Ellenberger showed the existence of a roughly vertical regional cleavage, distorted by reverse shear planes in the Lagrasse structure. A precise microstructural study by Cluzel (1977), summarized in Bogdanoff & Cluzel (1981), showed that both the initially vertical cleavage and an associated network of conjugate reverse microfaults were tilted in the flexure. He derived a relative chronology in which the regional cleavage and the related reverse faults were developed prior to the fold and the subsequent thrust faults.

The back of the structure is cut out by several ENE–WSW normal faults, which delimit the Miocene half-graben of Tournissan and are responsible for the tilting and collapse of the previous situation.

East of the Lagrasse village, the front of the structure is complicated by the superposition of three slices of Lower Ilerdian limestones resting on a horizontal foreland and overlain by the overturned beds of the Lagrasse fold forelimb (Fig. 3). This tectonic stack, the so-called 'La Cagalière' structure (Ellenberger 1967), is frontally wrapped in the Upper Ilerdian marls forming a kind of passive roof duplex. Into the 'La Cagalière' duplex, each slice is tilted to a steeper dip than the slice situated immediately beneath. This geometric pattern is characteristic of a progressive sequence towards the foreland in which the higher slices are carried 'piggy back' by the younger ones developing beneath them. We propose to link the development of the 'La Cagalière' duplex to the displacement of the Lagrasse fold unit, acting as a bulldozer (Geiser 1988), above a NW-vergent blind décollement-fault (Fig. 4a). Such an imbricate stack is indicative of difficulties in thrust propagation. The development of out-of-sequence forelimb thrusts on the back of the 'La Cagalière' duplex achieves the Pyrenean building of the Lagrasse structure.

Both the geometrical pattern and the deformation sequence described above cannot be explained by previous interpretations (Ellenberger 1967, Cluzel 1977). We propose a new interpretative cross-section, assuming constant area, plane strain and constant bedding thickness, in which the Lagrasse fold is related to the staircase geometry of a deep-seated thrust (Fig. 4). The unfolding of the Lower Ilerdian limestone layers involved in the 'La Cagalière' duplex has been used to set a first footwall cut-off line joining the upper ramp and the highest décollement level situated at the base of the Upper Ilerdian marls. The deeper structures are less constrained mainly because of the collapse of the back of the structure. We also favour an interpretation with two other décollement levels; an intermediate one at the base of the late Cretaceous deposits, and a basal one which is either within the basement or at the base of the Mesozoic deposits (Trias evaporites) if they exist. In the latter case, the basal ramp could reflect the northern limit of the Mesozoic basin.

In order to account for the structural evolution of the Lagrasse area, three major progressive deformation events can be defined:

(i) According to Cluzel, the first event led to the development of the regional vertical cleavage by layer parallel shortening (LPS) of the Cenozoic cover upon the Maastrichtian décollement level. Such a deformation may have been favoured by the existence of a regionally extensive network of vertical strike-slip faults, that could have acted like relative buttresses to displacement (Gillcrist *et al.* 1987).

Subsequently, a network of reverse conjugate fractures developed. These reverse faults are not distributed homogeneously over the entire Lagrasse area. They are preferentially developed on the present hangingwall of the major thrust and are less well developed over the autochthonous unit. This distribution is indicative of a

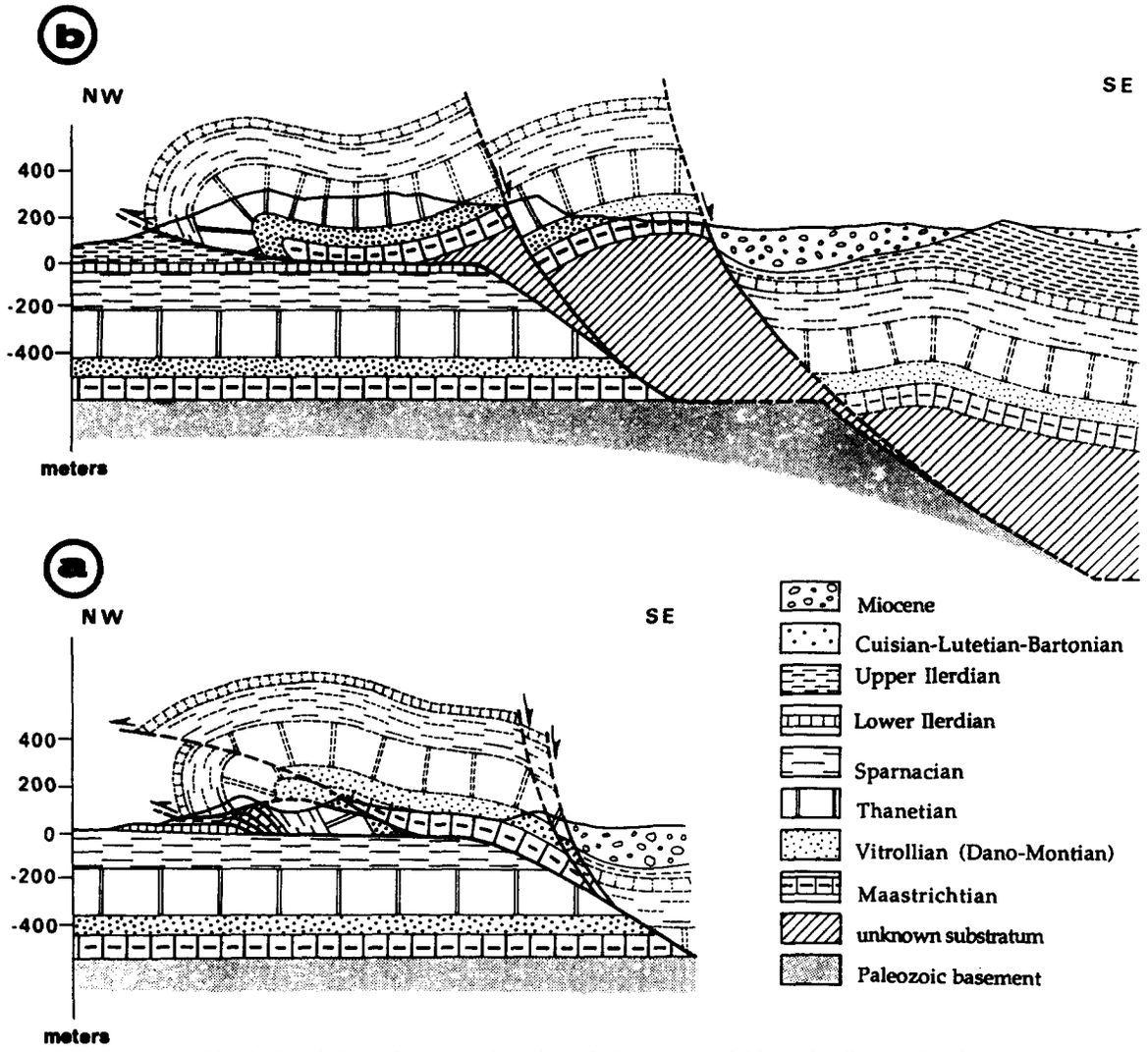

Fig. 4. Two balanced cross-sections through the Lagrasse fold (section lines on Fig. 2).

deformation gradient from the foreland towards the Lagrasse fold, related to an increase of the shortening intensity.

The amount of shortening due to this early pressure solution cleavage is difficult to estimate but it seems likely (cf. Hossack 1979) that this phenomenon accounts for a maximum of 20% shortening of the horizontal layers;

(ii) the second event is the ramp-related fold emplacement described above.

(iii) a later (Miocene) deformation phase induced the reactivation of the ramps and décollement levels as normal faults on the back of the structure producing a geometry of tilted blocks. This late extensional deformation will not be discussed in this paper.

METHODOLOGY

In order to define more precisely the deformation sequence, two kinds of analyses have been performed.

Analysis of fault slip data

The general kinematic framework of the studied area has been established by Cluzel (1977). He determined the bulk direction of shortening (NW–SE) and tectonic transport (towards the NW) using microfault population analysis. In order to define the different tectonic events and the style of the deformation, we have taken fault striation measurements at sites also sampled for magnetic fabric analysis.

Over the entire area, the mesoscopic faults are nearly parallel to the NE–SW strike of the major thrust-faults and of the Lagrasse fold axis. However, depending on the structural position, two associations have been distinguished and different analyses have been carried out accordingly.

A first group of sites exhibits the conjugate reverse faults which we interpret as the result of pure shear shortening during the LPS event. For these sites microfault population analyses have been performed using Carey's inversion algorithm (1979). This method is based on the hypothesis that striations are related to

independent and small displacements of rigid blocks and are parallel to the shear stress resolved on each fault plane. Inversion of the slip data gives the azimuths and the plunges of the principal axes of the stress tensor and a shape ratio calculated using the difference between the principal deviatoric stress values. When the deformation 'event' analysed in this way is predominant (or, obviously, when it is the only one recorded), we expect a direct relationship between finite strain ellipsoid and stress ellipsoid. If successive brittle deformations are observed and if partition between them is possible, the stress tensor, calculated for each population, is only representative of an incremental strain tensor.

A second set of sites is characterized by a close association of low-angle synthetic reverse and normal shear planes. Such typical geometry is found in zones of variable thickness across the thrust-faults and is indicative of non-coaxial deformation (Wiltschko *et al.* 1985, Wojtal 1986, Wojtal & Mitra 1986, Woodward *et al.* 1988, Guézou *et al.* 1991). In such a context, the use of the stress tensor axes calculation is not appropriate and is probably meaningless; fault slip data then provides only kinematic information.

Anisotropy of magnetic susceptibility

Magnetic fabric, derived from the analysis of anisotropy of magnetic susceptibility (AMS), reflects the statistically preferred orientation of grains and/or crystal lattices of all the minerals which contribute to the magnetic susceptibility (essentially ferro- and paramagnetic minerals). During depositional processes and compaction of sedimentary rocks and during subsequent deformation, fabric changes will be reflected in the AMS.

The principle of the method is as follows. In anisotropic materials, the low-field magnetic susceptibility may be described by a symmetric tensor of second order which relates the applied magnetic field to the induced magnetization of the material. It can be visualized as an ellipsoid characterized by principal axes $K_{max} > K_{int} > K_{min}$ which correspond to the eigenvectors of the susceptibility tensor. Orientation and intensity of the principal susceptibilities determine the geometric characteristics of the AMS ellipsoid. In order to define the shape of the ellipsoid, we have used the foliation ($F = K_{int}/K_{min}$) and lineation ($L = K_{max}/K_{int}$) parameters. Thus, in a L vs F plot, the points situated above the bisector represent prolate ellipsoids ($K_{max} \gg K_{int} \geq K_{min}$) and those situated below the bisector, oblate ellipsoids ($K_{max} \geq K_{int} \gg K_{min}$). A mean value of the degree of anisotropy, defined as the ratio $P = (K_{max}/K_{min})$, has been calculated for each site and is expressed as a percentage $[(P - 1) \times 100]$. We will use this parameter as an indicator of the degree of organization of the petrofabric only as far as the magnetic mineralogy and lithology remain invariant.

On the scale of a site, when the K_{min} axes are clustered, they correspond to the pole of the magnetic foliation plane. On the other hand, clustering of the K_{max} axes defines the magnetic lineation.

AMS studies were first used for sedimentological purposes in undeformed sediments to detect directions of palaeocurrents (Hamilton & Rees 1970, Argenton *et al.* 1975). Subsequently, in strongly deformed rocks (shales, slates), numerous studies have clearly shown a qualitative agreement between AMS and the finite strain ellipsoid (for example Kneen 1976, Kligfield *et al.* 1981, Borradaile 1988).

Comparison with natural deformed markers such as pebbles, concretions and reduction spots has led to local quantitative relationships (Kneen 1976, Hrouda 1979, Rathore 1979, Kligfield *et al.* 1981, Siddans *et al.* 1984, Hirt *et al.* 1988) but has also demonstrated that no universal quantitative correspondence exists. Nevertheless, the shape of the AMS ellipsoid is qualitatively indicative of the arrangement and/or deformed shape of the minerals contributing to magnetic susceptibility. Thus, when the magnetic mineralogy remains constant over all the sampled area, variations in the shape and orientation of the AMS ellipsoid indicate evolution of the petrofabric. These semi-quantitative relationships are particularly interesting in weakly deformed rocks where only microfault kinematic studies or technically complex experiments may give information about the microscale deformation. In such a context, AMS has proved to be a very useful kinematic indicator (Lee *et al.* 1990, Aubourg *et al.* 1991).

Measurements were made using a Kappabridge KLY-2 susceptibility bridge on standard oriented cylindrical samples. This process allows very accurate measurements of the magnetic susceptibility and consequently can detect an anisotropy of less than 1%.

SAMPLING, MAGNETIC MINERALOGY AND ORIGIN OF ANISOTROPY OF MAGNETIC SUSCEPTIBILITY

As mentioned above, magnetic fabric variations may be indicative of progressive deformation as long as the magnetic mineralogy and lithology remain constant over the whole sampling area. Therefore, we have investigated the same stratigraphic level at various key parts of the Lagrasse structure.

The Vitrollian Formation of Palaeocene age was selected because it displays both rather high susceptibilities and good strain markers. It consists mainly of red fluviatile calcareous silts containing various amounts of *Microcodium*.

A total of 150 oriented cores were collected in the Vitrollian level precisely located with respect to the Lagrasse structure (Fig. 2): in the foreland (sites A1 and A2), on the back of the Lagrasse structure (sites B1, B2, C and D), around the hinge of the frontal fold (sites E1, E2 and E3) and beneath the out-of-sequence forelimb thrusts (sites F and G). We will see that this structural distribution is also representative of the successive steps of the deformation history described above.

For each core, the bedding and cleavage attitudes have been determined in order to compare with the magnetic fabric.

The bulk susceptibility of the specimens varies between 10 and 50 $\times 10^{-6}$ S.I., the variation being due in part to differing amounts of diamagnetic calcite in the form of *Microcodium*. As the main component of the magnetic susceptibility (i.e. of the anisotropy) is due to paramagnetic and ferromagnetic phases and because recent work has shown that the paramagnetic contribution in sedimentary rocks may be as important as the ferromagnetic one (Rochette & Vialon 1984, Lamarche & Rochette 1987, Aubourg *et al.* 1991), the determination of the nature of each phase and their relative contribution is necessary in order to understand the origin of the magnetic fabric. In order to determine the relative proportion of each phase, we have analysed the hysteresis curves of representative specimens of the Vitrollian Formation, previously decarbonated (Fig. 5a). The hysteresis loops analyses were carried out using a Micromag Alternating Gradient Force Magnetometer with an applied field up to 1.8 T. At high fields (>1 T), the magnetic curves are perfectly reversible indicating that the induced magnetization is only of paramagnetic origin (the ferromagnetic component being negligible) with a significant slope. Thus, it shows that the paramagnetic contribution is not negligible at all in the low-field magnetic susceptibility.

In order to determine the nature of minerals, we have performed both magnetic and X-ray analyses.

The absence of complete saturation of the Isothermal Remanent Magnetization (IRM), even in applied fields as high as 2.8 T (Fig. 5b) and the relatively high value of the Remanent Coercitive Force, deduced from the hysteresis cycle (about 0.1 T), both strongly suggest that haematite is the main ferromagnetic mineral in the Vitrollian Formation. This is confirmed by X-ray diffractometry carried out on a powder from the same specimen as the one used for the hysteresis loop (Fig. 5c). In addition to quartz, calcite and haematite, the X-ray spectrum also shows a large amount of clay minerals such as kaolinite and illite. These paramagnetic minerals are probably responsible for an important part of the low-field magnetic susceptibility.

In any case, haematite and clay minerals have a dominant magnetocrystalline anisotropy with a minimum susceptibility perpendicular to their basal plane and a maximum susceptibility within this plane. Thus, the anisotropy of magnetic susceptibility of the Vitrollian samples may be interpreted in terms of preferred orientation of the crystal lattice of clay minerals and haematite. The magnetic foliation, where it exists, corresponds to the plane in which the basal planes of the minerals tend to align. In this case it is not surprising that the magnetic foliation coincides either with the bedding plane (Kligfield *et al.* 1981, Lowrie & Hirt 1987) or with the cleavage (Kneen 1976, Kligfield *et al.* 1981). The existence of a magnetic lineation within the foliation is more questionable. Indeed, there is no preferential axis of maximum susceptibility within the basal planes of the

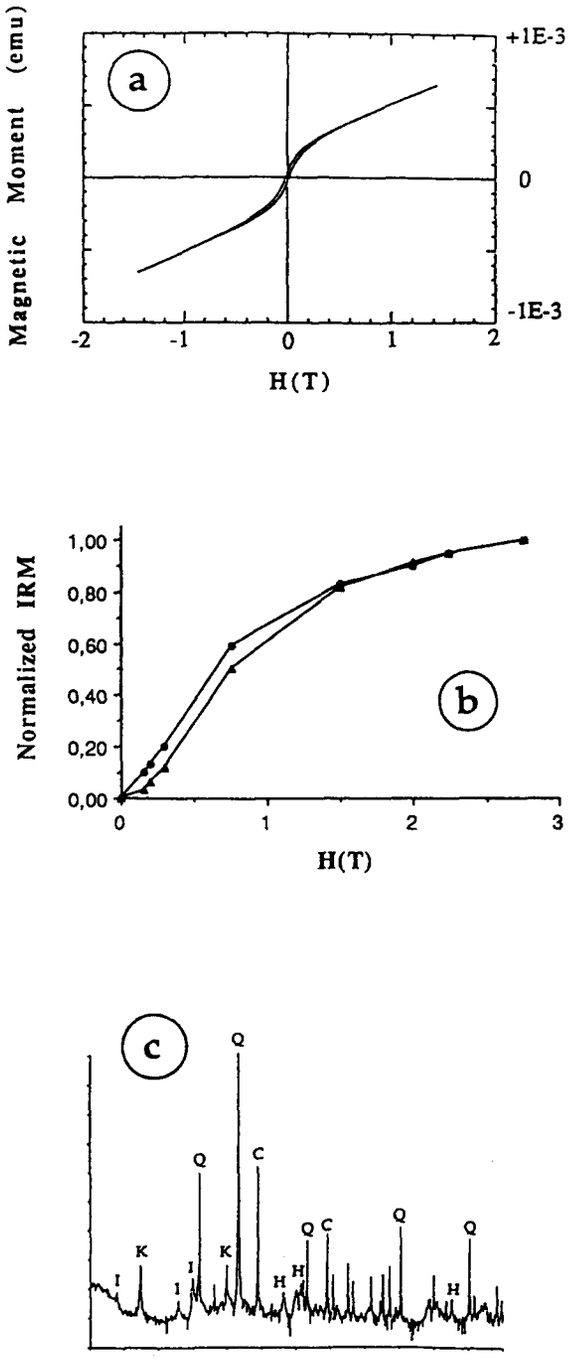

Fig. 5. (a) Hysteresis curve carried out on a representative specimen of Vitrollian red fluviatile silts. (b) Representative normalized curves of acquisition of Isothermal Remanent Magnetization. (c) X-ray diffractometry spectrum obtained on a representative specimen of Vitrollian. C, calcite; Q, quartz; K, kaolinite; I, illite; H, haematite.

cristal lattices of haematite and clays. However, in deformed rocks with AMS due to magnetocrystalline effects, it has been shown that the magnetic lineation in general coincides with the direction of extension of the strain ellipsoid (Kneen 1976, Kligfield *et al.* 1981). Two types of mechanism may be invoked:

—the first one is due to a slight shape anisotropy related to the oriented recrystallization, during the deformation, of minerals with a major magnetocrystalline anisotropy;

—in the second more realistic mechanism, the inter-

section of the statistically preferentially oriented basal planes (i.e. magnetic foliation), determines a zonal axis, which in turn represents the direction of extension of the strain ellipsoid. Thus, in the case of the Vitrollian rocks, this lineation could be interpreted as the result of a subtle microscopic crenulation of clay and haematite basal planes within the cleavage plane. Such structural pattern may be compared with the crenulation which frequently occurs parallel to the stretching direction during ductile deformation.

RESULTS AND DISCUSSION

In all the sites, the magnetic fabric can be related to strain indicators so that its tectonic origin remains unquestionable. Depositional and/or compactional fabrics have clearly been reworked. Thus, the magnetic fabric may be explained only in terms of a deformation-related reorganization.

As shown by the L/F synthetic diagram (Fig. 6), the shape of the AMS ellipsoid is oblate in all cases except for some samples from site A1 which are weakly prolate. However, significant differences appear in the lineation and foliation parameters of the different sites supporting the idea that each of them represents a different stage in the progressive deformation of the Lagrasse fold.

Sites A1 and A2, both situated in the foreland of the Lagrasse fold, are characterized by a subhorizontal bedding and a rough vertical cleavage trending ENE–WSW. At these sites, the mean degree of anisotropy is weak (about 2%). Although the tectonic pattern is similar for both sites, they exhibit slight differences in their magnetic fabrics (Fig. 7). Site A2 shows a well defined magnetic foliation (defined by clustering of K_{min}), which coincides with the vertical cleavage measured in the field. No preferred orientation of K_{max} and K_{int} is observed in this plane. K_{min} lies horizontally within the bedding and trends NNW–SSE parallel to the regional shortening direction. The magnetic pattern

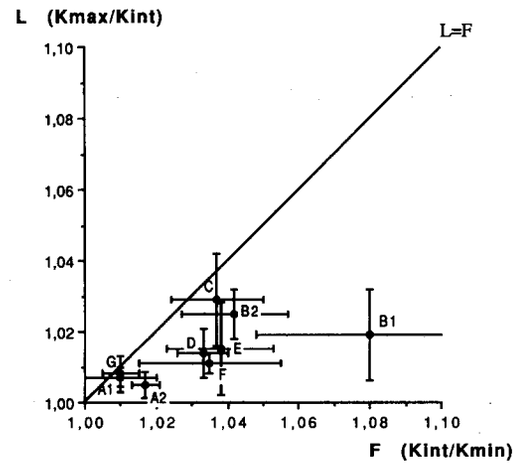

Fig. 6. Synthetic diagram of the mean shape parameters of the ellipsoid of anisotropy of magneticd susceptibility at each site. L (lineation parameter) = K_{max}/K_{int}; F (foliation parameter) = K_{int}/K_{min}.

observed in site A1 is more complex. Two populations of specimens can be distinguished. Part of the samples are characterized by an AMS ellipsoid weakly prolate with K_{max} parallel to the cleavage–bedding intersection direction (about 260°N horizontal) and K_{int} and K_{min} distributed within the perpendicular plane. The second group of samples exhibits the same magnetic pattern as site A2 with a magnetic foliation parallel to the cleavage plane. The subtle pencil structure fabric, observed for the first group of specimens, can be interpreted as an interference between the previous depositional fabric and the forming tectonic fabric, parallel to cleavage (Borradaile & Tarling 1981). The association of these two types of magnetic fabric within the same site represents a transitional state indicative of an evolution in the arrangement of haematite and clay minerals basal planes within the bedding and cleavage discontinuities, the latter becoming progressively dominant. Thus, the mechanism of cleavage formation during the early event of layer parallel shortening seems to imply the remobilization of the calcitic matrix by pressure solution coeval with the passive displacement and rotation of haematite and clay minerals within the cleavage plane. This agrees with Cluzel's results (1977) which were obtained by SEM analysis on specimens of Vitrollian rocks from the Lagrasse area.

Sites B1 and B2, situated on the back of the Lagrasse fold close to the Tournissan normal fault, exhibit the same tectonic framework as sites A1 and A2 (the trend of cleavage being, however, more NE–SW) but with an additional set of conjugate reverse microfaults at site B2 (Fig. 8). Percentages of anisotropy of about 10 and 7% suggest that the magnetic fabric is more intense than in the foreland. At both sites, the AMS ellipsoid is characterized by a magnetic foliation, still parallel to the cleavage (Figs. 9 and 10a). At site B2, a magnetic lineation (cluster of K_{max}) appears within the vertical foliation plane (Fig. 10a). This well defined magnetic lineation, roughly perpendicular to the intersection of bedding and cleavage, is not detectable in the field. However, it is responsible for a coarse vertical pencil structure as observed by Cluzel (1977). We have determined, using the Carey's algorithm (1979), the azimuths and plunges of the principal axes of the stress tensor responsible for brittle deformation. The σ_1, σ_2 and σ_3 axes ($\sigma_1 > \sigma_2 > \sigma_3$) are strictly parallel to the AMS ellipsoid axes K_{min}, K_{int} and K_{max}, respectively (Fig. 10b). Such a result provides a good argument for the confident interpretation of the magnetic lineation as the extension direction of the strain ellipsoid.

The whole deformation analysed at site B2 can be related to layer parallel shortening under a pure shear regime. With respect to sites A1, A2 and B1, the coeval occurrence of the magnetic lineation and the conjugate reverse faults is indicative of an increase in the LPS intensity in the vicinity of the location of the future thrust. The vertical stretching suggests that lateral escape would be regionally difficult.

The present position of sites B1 and B2 requires that they suffered upward and then downward bending when

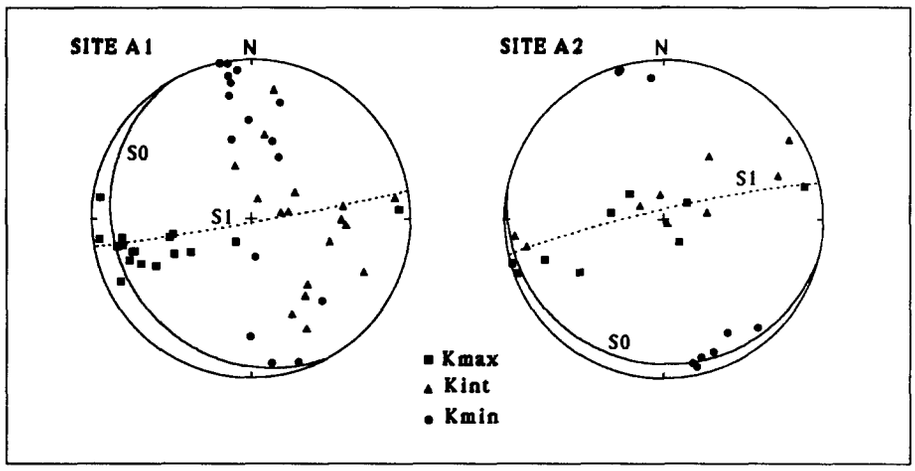

Fig. 7. Magnetic fabric in the foreland of the Lagrasse fold (sites A1 and A2) plotted relative to geographic co-ordinates. S_0 bedding; S_1, cleavage (lower-hemisphere equal-area projection).

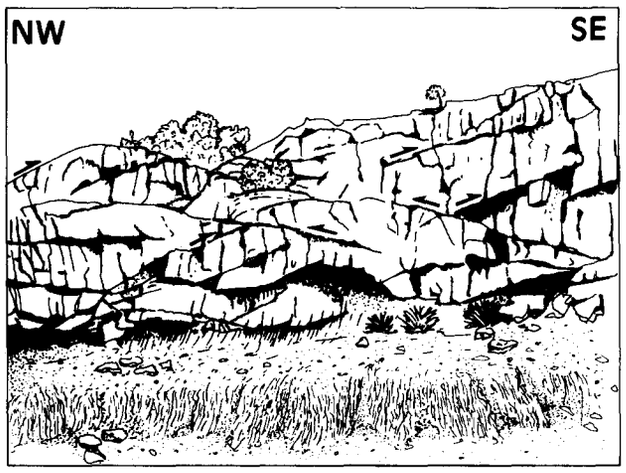

Fig. 8. The vertical cleavage and the conjugate reverse faults at Terres Rouges (site B2 drawn from a photograph).

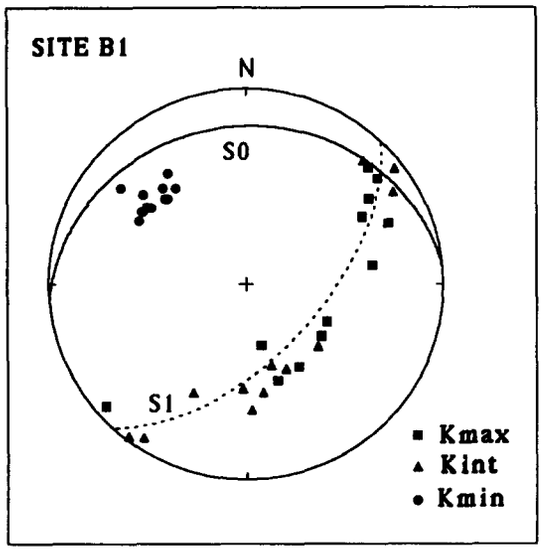

Fig. 9. Magnetic fabric at site B1. The slight tilting of bedding is linked to the late normal faulting.

they passed over the ramp. It is worth noting that there are no measureable records of these phenomena.

Other sites (C and D) in a similar structural position but closer to the frontal kink (Fig. 2) exhibit the same tectonic and magnetic pattern as site B2 with a slight tilting of the cleavage plane and magnetic foliation with respect to the bedding (Fig. 11). That may be an imprint of a slight global shearing linked to the displacement of the hangingwall on the blind major décollement fault. However, there is no strong evidence for such an event. The pre-existing magnetic lineation would thus indicate the direction of shear, i.e. of displacement.

Around the hinge of the frontal fold, we have collected 31 cores distributed in three sites situated, respectively, in the subhorizontal roof limb (site E1), within the hinge itself (site E3) and in the upper part of the vertical forelimb (site E2) (Fig. 12). The previous cleavage and associated conjugate reverse faults are rotated (Fig. 13) so that they always keep the same relationship with bedding whatever their position in the fold. In the forelimb, additional low-angle S-dipping reverse faults appear. These faults deform the cleavage so that it is clear that they cross-cut the early emplaced fold. We interpret them as being due to the out-of-sequence thrusting event evident (and more developed) in the 'La Cagalière' area.

'Stress tensors' have been calculated from slip data on the rotated reverse faults only (Fig. 12). It appears that the compression and extension directions related to the LPS event suffered exactly the same rotation as the bedding. Such geometric relationships may suggest that only rigid-body rotation occurred during the fold formation. The magnetic fabric analysis allows us to complete this macroscopical approach.

Whatever the position in the fold, the magnetic foliation is well defined. It is still parallel to the cleavage in the subhorizontal limb and in the hinge. In the vertical limb, by contrast, the magnetic foliation and the cleavage measured in the field are not coincident. The apparent rotation of the magnetic foliation is less (by about 20°) than the rotation suffered by the cleavage (Fig. 12). This means that the macroscopic cleavage inherited

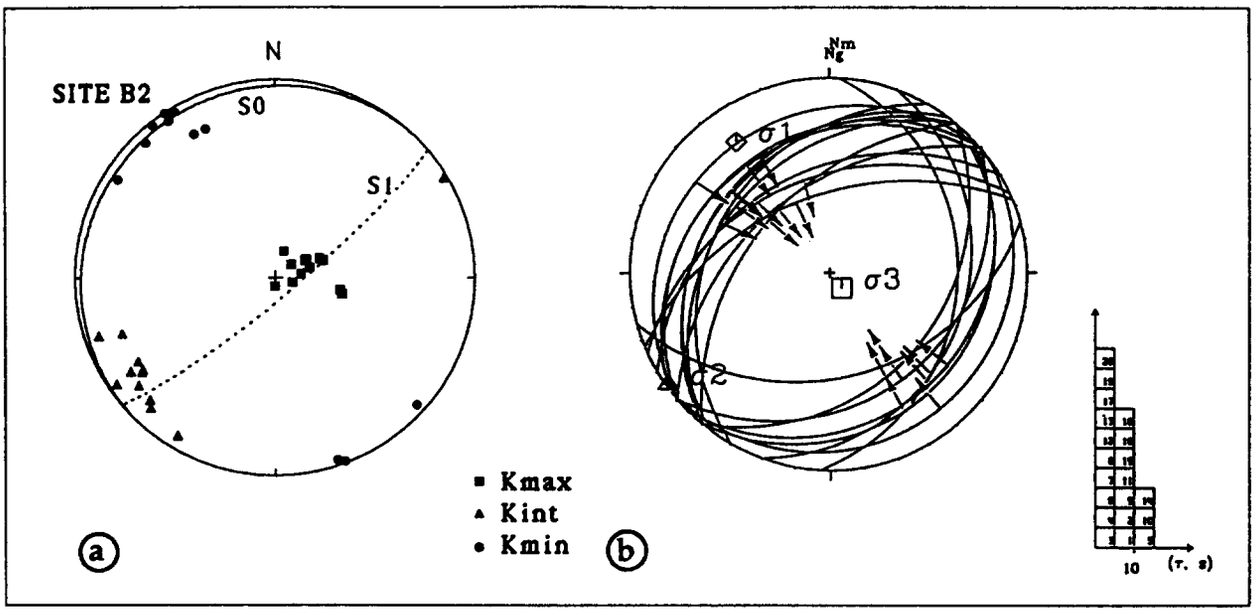

Fig. 10. Magnetic fabric and fault measurements at site B2. Arrows on the fault traces correspond to the measured striation 's'. σ_1, σ_2 and σ_3 refer to the computed principal stress directions. The histogram gives the deviation between measured (s) and predicted (τ) slip vectors for all fault planes.

from the LPS event is no longer a principal strain plane or, in other words, that internal deformation occurred during folding.

The magnetic lineation is less well defined at each of these sites than at sites B2, C and D. Furthermore, with respect to these sites, the K_{max} axes tend to be rotated from the previous subvertical position toward the bedding–cleavage intersection. The differences with the magnetic pattern linked to the layer parallel shortening (site B2) suggest that frontal folding is associated with stretching parallel to the fold axis and internal flattening. Such a longitudinal stretching suggests that lateral escape which was impossible during the LPS event was favoured during the fold emplacement.

We emphasize the important reorganization of the magnetic fabric that occurred in the frontal fold. Such a reorganization is significant of the large internal deformation which occurred during frontal folding. During this deformation, the cleavage and conjugate reverse faults acted as passive markers retaining a memory of the LPS deformation stage. There is no development of a new macroscopic cleavage related to folding.

The last group of sites (sites F and G) is situated immediately beneath the out-of-sequence thrusts in the 'Cluse de Ribaute' and 'Col Rouge' areas (Fig. 2). These thrust faults are accompanied by intense penetrative deformation concentrated in zones extending about 10 m beneath the thrust plane. Bedding and previous tectonic planes have been destroyed within these deformation zones and a new cleavage associated with shear planes has developed. Cleavage forms an angle of about 30° with the thrust plane. Most of the shear planes are low-angle (dip <30°) reverse and normal faults dipping, respectively, to the SE and NW (Fig. 14b). The slip along this plane is synthetic to the thrust-sheet transport (about 310°N). Scarce high-angle antithetic and synthetic reverse faults are also present. Such an association, comparable with the pattern found in defor-

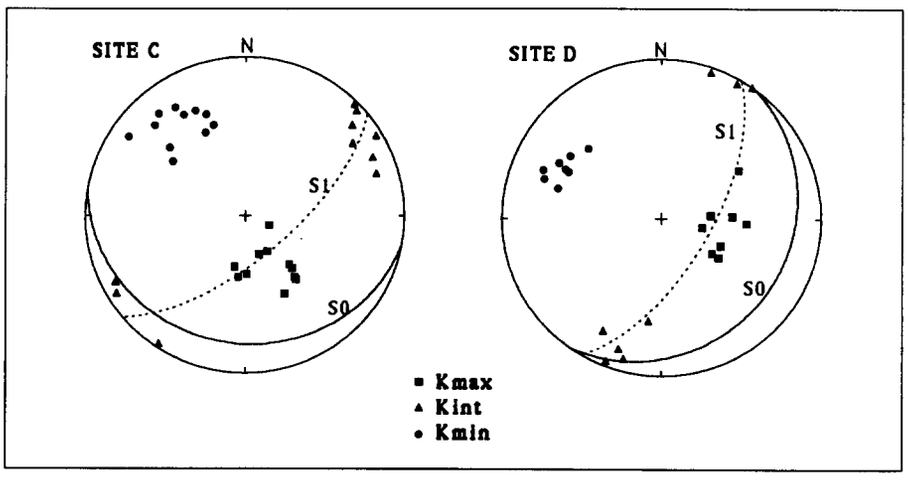

Fig. 11. Magnetic fabric at sites C and D (see explanation in text).

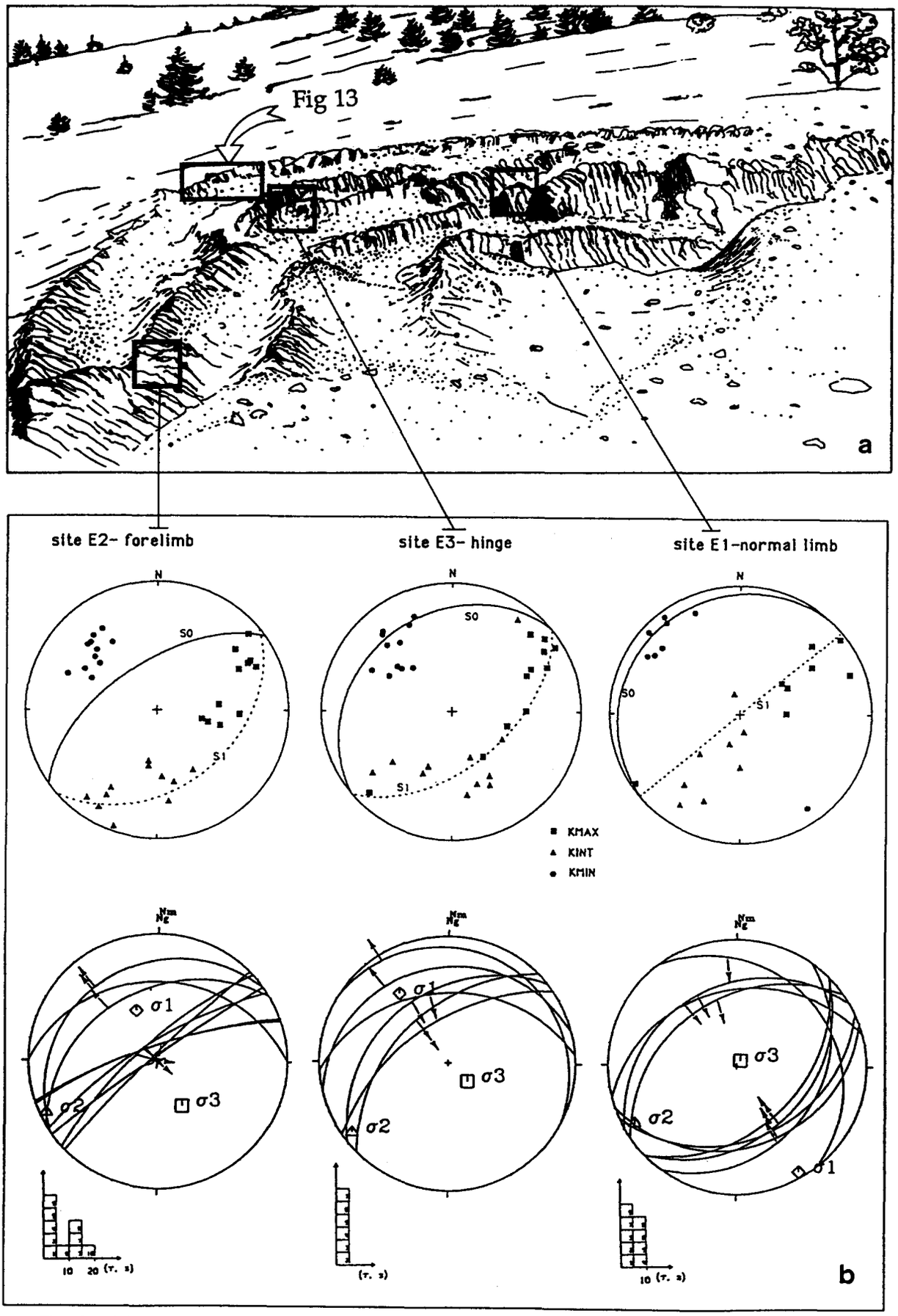

Fig. 12. (a) Sketch view of the frontal fold hinge at 'La Cluse de Ribaute' area showing the tilting of the LPS-related cleavage. Squares refer to the sampled sites E1, E2 and E3 and the rectangle to the location of the Fig. 13. (b) Magnetic fabric and microfault measurements at sites E1, E2 and E3. Same legend as Fig. 10. The faults formed during the LPS event are subsequently tilted.

Fig. 13. Sketch view (from a photograph) showing the tilting of the conjugate reverse faults in the hinge of the frontal fold of the Lagrasse structure.

mation zones of numerous thrust systems, is indicative of a non-coaxial strain regime as discussed above. On the AMS diagrams (Fig. 14a), the principal susceptibility directions are clearly more scattered compared to results from sites situatied at the back of the Lagrasse fold. The degree of anisotropy (5 and 3%, respectively) as well as the shape parameters (L, F) show that the magnetic fabric is not strongly devleoped. In site F, the magnetic foliation coincides roughly with cleavage. In site G, the magnetic foliation is poorly defined so that it is difficult to compare cleavage. However, in both cases, a weak magnetic lineation may be inferred which tends

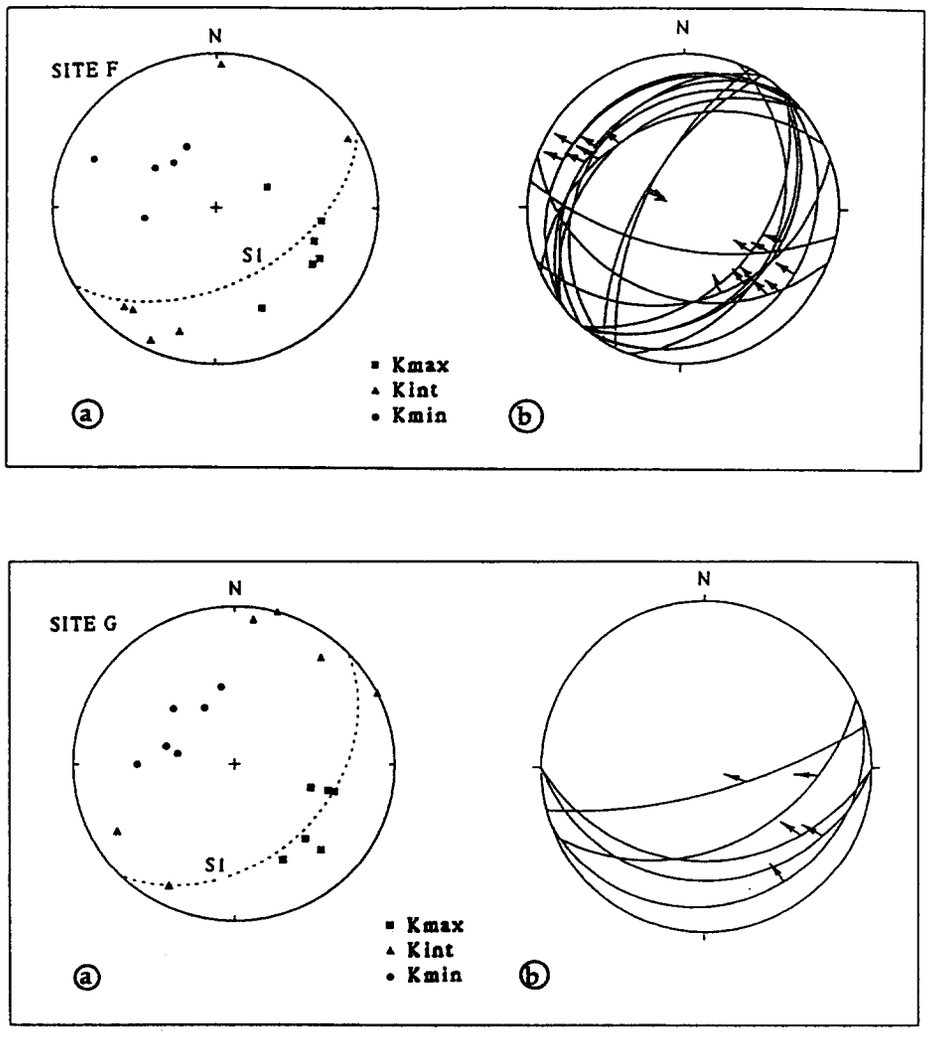

Fig. 14. Magnetic fabric and fault measurements at sites F and G. See explanation in text.

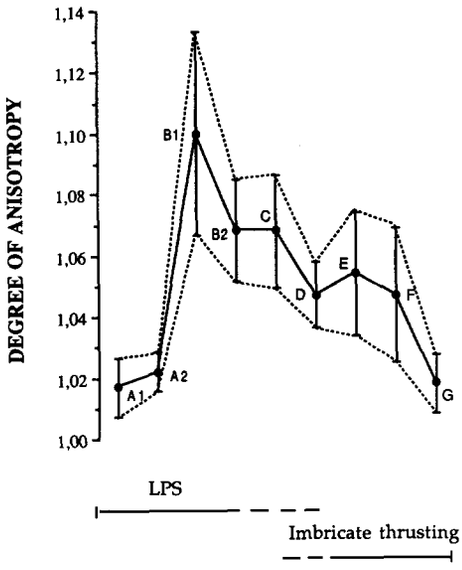

Fig. 15. Evolution of the mean degree of anisotropy (K_{max}/K_{min}) at each site during the evolution of the Lagrasse structure. Each letter refers to one site except E which refers to the sites E1, E2 and E3.

to be parallel to the tectonic transport determined by slip directions on shear planes (Fig. 14).

The superimposition of a global non-coaxial strain regime, due to the out-of-sequence thrusting, induced once again a reorganization of the magnetic fabric including the development of a magnetic lineation parallel to the tectonic transport direction.

In order to discuss the chronological evolution of the magnetic fabric intensity, we show in Fig. 15 the mean degree of anisotropy calculated for each site vs their degree of deformation. From sites A1 and A2 situated in the foreland which we consider to represent a first stage in the deformation, we observe first an increase in the degree of anisotropy toward the site B1, B2 and C and then an overall decrease up to G. The most intense magnetic fabric corresponds to the LPS event (sites B1 and B2). Subsequent deformation events have tended to reorganize the fabric without producing the same degree of arrangement. This highlights the fact that the degree of anisotropy does not reflect the deformation intensity (discussion in Rochette 1988).

Such a complex history (path shown in Fig. 15) emphasizes the difficulties in global fabric interpretation when it is related to different stages of deformation. However, if each increment is preserved, as in the studied example, the anisotropy of magnetic susceptibility measurements provides a very efficient tool for documenting steps in the progressive deformation.

CONCLUSIONS

Two main mechanisms have acted successively during thrust-sheet motion of the Lagrasse structure (Fig. 16).

The first one resulted from a differential layer parallel shortening between a 'ductile' hangingwall (the Meso-Cenozoic sequence) and a more rigid footwall (the Palaeozoic basement). This mechanism was responsible

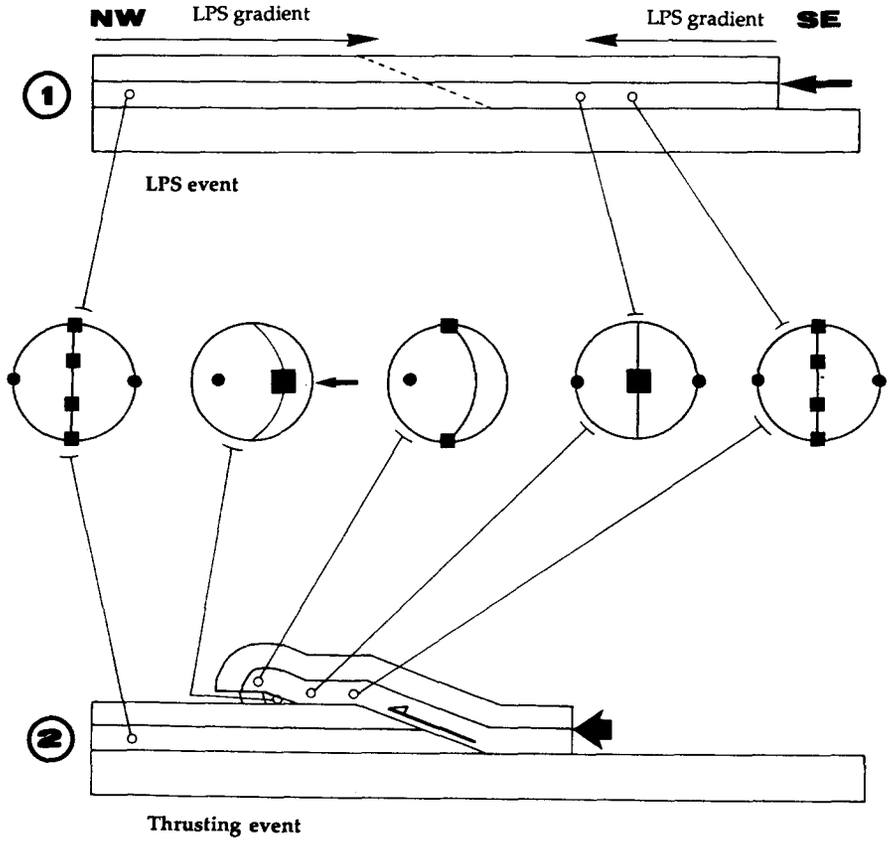

Fig. 16. Synthetic diagram showing the evolution of the magnetic fabric during thrust-sheet motion of the Lagrasse structure. Black squares and circles represent, respectively, the K_{max} and K_{min} directions of the AMS ellipsoid.

for major internal deformation (formation of a regional vertical cleavage by pressure solution with migration and preferred alignment of the clay minerals and haematite within the cleavage) with only minor displacements. The development of a vertical magnetic lineation within the cleavage plane, and conjugate reverse faults in the internal part of the structure, provides evidence supporting a gradual increase in the LPS intensity.

The second mechanism resulted from the failure of the Meso-Cenozoic sequence in the zone of maximum shortening during the LPS event and led to the development of imbricate thrusting upon a blind décollement fault (and related folding). This mechanism was responsible for a major rigid-body displacement with distortion localized only within the forelimb part of the structure. Whereas the rocks involved in the frontal fold apparently suffered only rigid-body rotation, an important reorganization of the magnetic fabric is observed. Around the hinge of the fold, the magnetic lineation rotated from its previous vertical position to the bedding–cleavage intersection direction parallel to the fold axis. We interpret this first reorganization as a result of flattening and longitudinal stretching during folding. During the out-of-sequence forelimb thrusting, the magnetic lineation swung once again and became parallel to the northwestward tectonic transport direction. This reorganization is related to the simple shear deformation characteristic of thrust zones as recently shown empirically on some nappes of the Alps (Lamarche & Rochette 1987) and theoretically on mathematical models (Hrouda 1991).

It is worth noting that this deformation scheme is only reliable because of the existence of a very special formation (Vitrollian levels) which preserves both magnetic fabric and structural indicators. Even if the surrounding rocks appear completely undeformed, they suffered exactly the same deformation path. This is the reason why we believe that internal distortion and particularly the effects of LPS are generally underestimated in shortening calculation. Attention must be paid to this point before any palinspastic restoration is attempted. Further studies in different types of structures, lithologies and magnetic mineralogies are needed to complete this deformation scheme in foreland fold–thrust structures.

Acknowledgements—The authors wish to thank R. Manganne for his active help in the field, G. Roche (CNRS URA 1369) for the drawings, C. Jehanno (C.F.R.) for the X-ray diffractometry, and R. Weeks and E. Pickett for comments and improving the English. We are also grateful to R. Kligfield, F. Hrouda and R. J. Lisle for their constructive comments on the manuscript. One of the authors (O. Averbuch) gratefully acknowledges a grant from the French Atomic Energy Commission (CEA). This is a C.F.R. contribution No. 1217.

REFERENCES

Argenton, H., Bobier, C. & Polvèche J. 1975. La mesure de l'anisotropie de susceptibilité magnétique dans les flyschs: application à la recheche des paléocourrants. *Sediment. Geol.* **14**, 149–167.

Aubourg, C., Rochette, P. & Vialon, P. 1991. Subtle stretching lineation revealed by magnetic fabric of Callovian–Oxfordian black shales (French Alps). *Tectonophysics* **185**, 211–223.

Barrabé L. 1922. Sur la présence de nappes de charriage dans les Corbières orientales. *C. r. Acad. Sci.* **175**, 1081.

Bogdanoff, S. & Cluzel, D. 1981. Un exemple de schistosité antérieure au plissement: la schistosité de l'avant-pays de la nappe des Corbières (Aude, France). *Bull. Soc. géol. Fr.* **23**, 361–366.

Borradaile, G. J. 1988. Magnetic susceptibility, petrofabrics and strain. *Tectonophysics* **156**, 1–20.

Borradaile, G. J. & Tarling, D. 1981. The influence of deformation mechanisms on magnetic fabrics in weakly deformed rocks. *Tectonophysics* **77**, 151–168.

Boyer, S. E. & Elliott, D. 1982. Thrust systems. *Bull. Am. Ass. Petrol. Geol.* **66**, 1196–1230.

Carey, E. 1979. Recherche des directions principales de contraintes associées au jeu d'une population de failles. *Rev. Geogr. phys. Geol. dyn.* **21**, 57–66.

Cluzel, D. 1977. Etude microtectonique de l'avant-pays de la Nappe des Corbières orientales (Aude, France). Unpublished these 3eme Cycle, Université de Paris Sud Orsay.

Coward, M. P. & Kim, J. H. 1981. Strain within thrust sheets. In: *Thrust and Nappe Tectonics* (edited by McClay, K. & Price, N. J.). *Spec. Publs geol. Soc. Lond.* **9**, 275–292.

Dahlstrom, C. D. A. 1969. Balanced cross-sections. *Can. J. Earth Sci.* **6**, 743–757.

Ellenberger, F. 1967. Les interférences de l'érosion et de la tectonique tangentielle tertiaire dans le Bas-Languedoc; note sur les charriages cisaillants. *Rev. Géogr. phys. Géol. dyn.* **9**, 87–142.

Ellenberger, F., Plaziat, J. C., Freytet, P., Jaffrézo, M. Charrière, A., l'Homer, A., Legrand-Lespinasse, N., Huguet, J., Bessière, G. & Berger, G. 1985. Carte géologique de la France à 1/50000. Feuille de Capendu. Bureau de Recherches Géologiques et Minières, Orleans, France.

Evans, M. A. & Dunne, W. M. 1991. Strain factorization and partitioning in the North Mountain thrust sheet, central Appalachians, U.S.A. *J. Struct. Geol.* **13**, 21–35.

Fischer, M. W. & Coward, M. P. 1982. Strains and folds within thrust sheets: an analysis of the Heilam sheet, northwest Scotland. *Tectonophysics* **88**, 291–312.

Freytet, P. 1970. Les dépôts continentaux et marins du Crétacé supérieur et les couches de passage à l'Eocène en Languedoc. Unpublished thèse Sci., Université de Paris Sud Orsay.

Geiser, P. A. 1988. The role of kinematics in the construction and analysis of geological cross-sections in deformed terranes. In: *Geometries and Mechanisms of Thrusting* (edited by Mitra, G. & Wojtal, S.). *Spec. Pap. geol. Soc. Am.* **222**, 47–76.

Gillcrist, R., Coward, M. & Mugnier, J. L. 1987. Structural inversion and its control: examples from the Alpine foreland and the French Alps. *Geodinamica Acta* **1**, 5–34.

Guézou, J. C., Frizon de Lamotte, D., Coulon, M. & Morel, J. L. 1991. Structure and kinematics of the Prebetic Nappe Complex (southern Spain): definition of a "Betic Floor Thrust" and implications in the Betic-Rif orocline. *Annales Tectonicae* **5**, 32–48.

Hamilton, N. & Rees, A. J. 1970. The use of magnetic fabric in paleocurrent estimation. In: *Palaeogeophysics* (edited by Runcorn, S. K.). Oxford, 445–463.

Hirt, A. M. Lowrie, W., Clendenen, W. S. & Kligfield, R. 1988. The correlation of magnetic anisotropy with strain in the Chelmsford Formation of the Sudbury Basin, Ontario. *Tectonophysics* **145**, 177–189.

Hossack, J. R. 1979. The use of balanced cross-sections in the calculation of orogenic contraction: a review. *J. geol. Soc. Lond.* **136**, 705–711.

Hrouda, F. 1979. The strain interpretation of magnetic anisotropy in rocks of the Nizky Jesenik Mountains (Czechoslovakia). *Sb. Geol. Ved., UG* **16**, 27–62.

Hrouda, F. 1991. Models of magnetic anisotropy variations in sedimentary thrust sheets. *Tectonophysics* **185**, 203–210.

Kissel, C., Barrier, E., Laj, C. & Lee, T. Q. 1986. Magnetic fabric in "undeformed" marine clays from compressional zones. *Tectonics* **5**, 769–781.

Kligfield, R., Owens, W. H. & Lowrie, W. 1981. Magnetic susceptibility anisotropy, strain and progressive deformation in Permian sediments from the Maritime Alps (France). *Earth Planet. Sci. Lett.* **55**, 181–189.

Kneen, S. 1976. The relationship between the magnetic and strain fabrics of some haematite-bearing Welsh slates. *Earth Planet. Sci. Lett.* **31**, 413–416.

Lamarche, G. & Rochette, P. 1987. Microstructural analysis and origin of lineations in the magnetic fabric of some Alpine slates. *Tectonophysics* **139**, 285–293.

Lee, T. Q., Kissel, C., Laj, C., Horng, C. S. & Lue, Y. T. 1990.

Magnetic fabric analysis of the Plio-Pleistocene sedimentary formations of the Coastal Range of Taiwan. *Earth Planet. Sci. Lett.* **98**, 23–32.

Lowrie, W. & Hirt, A. M. 1987. Anisotropy of magnetic susceptibility in the Scaglia Rossa pelagic limestone. *Earth Planet. Sci. Lett.* **82**, 349–356.

Plaziat, J. C. 1984. Le domaine pyrénéen de la fin du Crétacé à la fin de l'Eocène. Stratigraphie, paléo-environnements et évolution paléogéographique. Unpublished thèse Sci., Université de Paris Sud Orsay.

Rathore, J. S. 1979. Magnetic susceptibility anisotropy in the Cambrian Slate Belt of North Wales and correlation with strain. *Tectonophysics* **53**, 83–97.

Rochette, P. 1988. La susceptibilité anisotrope des roches faiblement magnétiques: origine et applications. Unpublished thèse Sci., Université J. Fourier Grenoble.

Rochette, P. & Vialon, P. 1984. Development of planar and linear fabrics in Dauphinois shales and slates (French Alps) studied by magnetic anisotropy and its mineralogical control. *J. Struct. Geol.* **6**, 33–38.

Roure, F., Choukroune, P., Berastegui, X., Munoz, J.A., Villien, A., Matheron, P., Bareyt, M., Seguret, M., Camara, P. & Deramond, J. 1989. Ecors deep seismic data and balanced cross-sections: geometric constraints on the evolution of the Pyrenees. *Tectonics* **1**, 41–50.

Sanderson, D. J. 1982. Models of strain variation in nappes and thrust sheets: a review. *Tectonophysics* **88**, 201–233.

Siddans, A. W. B., Henry, B., Kligfield, R., Lowrie, W., Hirt, A. M. & Percevault, M. N. 1984. Finite strain patterns and their significance in Permian rocks of the Alpes Maritimes (France). *J. Struct. Geol.* **4**, 339–368.

Suppe, J. 1983. Geometry and kinematics of fault-bend folding. *Am. J. Sci.* **283**, 684–721.

Wiltschko, D. V., Medwedeff, D. A. & Millson, H. E. 1985. Distribution and mechanisms of strain within rocks on the northwest ramp of Pine Mountain block, southern Appalachian foreland: A field test of theory. *Bull. geol. Soc. Am.* **96**, 426–435.

Wojtal, S. 1986. Deformation within foreland thrust sheets by populations of minor faults. *J. Struct. Geol.* **8**, 341–360.

Wojtal, S. & Mitra, G. 1986. Strain hardening and strain softening in fault zones from foreland thrusts. *Bull. geol. Soc. Am.* **97**, 674–687.

Woodward, N. B., Wojtal, S., Paul, J. B. & Zadins, Z. Z. 1988. Partitioning of deformation within several external thrust zones of the Appalachian orogen. *J. Geol.* **96**, 351–361.